Chemical Physics 370 (2010) 215–222

Contents lists available at ScienceDirect

Chemical Physics

journal homepage: www.elsevier.com/locate/chemphys

Vibration correlation function formalism of radiative and non-radiative rates for complex molecules

Qian Peng [a], Yingli Niu [a], Chunmei Deng [a], Zhigang Shuai [a,b,*]

[a] Key Laboratory of Organic Solids, Beijing National Laboratory for Molecular Science (BNLMS), Institute of Chemistry, Chinese Academy of Sciences, 100190 Beijing, PR China
[b] Department of Chemistry, Tsinghua University, 100084 Beijing, PR China

ARTICLE INFO

Article history:
Received 26 February 2010
In final form 4 March 2010
Available online 1 April 2010

Keywords:
Radiative rate
Non-radiative rate
Vibration correlation function method
Duschinsky rotation
Herzberg–Teller effect

ABSTRACT

General radiative and non-radiative rates formalisms are derived using the vibration correlation function method for the transition from the excited singlet to ground singlet states by considering the Duschinsky rotation and Herzberg–Teller effects at finite temperature. For the non-radiative transition process, the conventional assumption of (single) "promoting-mode" is abandoned and a promoting-mode free formula is presented. Using this new rate formalism, we re-examine the well-established photophysical properties of anthracene. Both the calculated radiative and non-radiative rates are in good agreement with the available experimental measurements and previous theoretical values. Furthermore, we rationalize the exotic aggregation induced emission phenomenon in 9-[(o-Aminophenyl)phenylmethylene]-9H-fluorene molecule: the roles of low-frequency phenyl ring twist motions and their Duschinsky mode mixings are found to be crucial, especially for the temperature dependence. The present rate theory can quantitatively describe the excited-states dynamic processes in large molecules and is a powerful tool for the design of new high-efficiency light-emitting materials.

1. Introduction

Molecular fluorescence efficiency is important to design organic light-emitting and sensing materials, which have attracted much attention recently due to far-ranging applications as luminescent and sensory materials in optical display, environmental protection, and biomedical imagining [1]. Theoretically, molecular fluorescence efficiency is determined by the competition between radiative decay and non-adiabatic decay from electronically excited state to ground state [2].

The radiative rate from a given excited singlet state to the ground state can be obtained by integrating over the optical emission spectrum. For a complex molecule, by and large, the rate formalism is based on harmonic approximation and when the ground state and the excited state potential energy surfaces are different, Duschinsky rotation effects (DRE) is considered. Here, the theoretical evaluation involves a large number of multidimensional Franck–Condon integrals (FCIs). Standard algorithms relying on recurrence relations between the FCIs [3–11] requires formidable computational efforts with increasing system size, especially worse when vibrational modes are mixing. In practice, only a few modes with dominant contributions to FCIs are selected, and the transition is always assumed to start from the lowest vibration state ($T = 0$ K) [12]. Progresses have been made in developing efficient and accurate techniques to calculate FCIs. Yan and Mukamel have proposed a Green's function formalism both for absorption and emission spectra with DRE [13]. Grimme et al. firstly constructed the block-diagonal model Duschinsky rotation matrix with a set of approximate modes replacing the exact ones, and calculated the FCIs separately for the blocks by discarding all the modes below threshold, and then the total FCIs is obtained by direct multiplication [14,15]. Barone and co-workers presented an approach which can automatically select the relevant vibronic contributions to the spectrum until the spectrum converged [16–18]. Different from the above sum-over-states methods, the vibration correlation function approach was adopted to derive the FCIs with DRE by Pollak and co-workers [19–21]. The vibration correlation function method can give a full analytic formalism and all the vibrational modes are considered. In this work, we extend the vibration correlation function formalism to the radiative rate with Herzberg–Teller (HT) effect at finite temperature, in addition to DRE.

In the non-radiative decay process, the electronic energy of molecule in higher electronic excited state (say the first excited state S_1) is converted into the vibrational energy of the molecule or the environment, as the molecule relaxes into a lower ground electronic state (S_0) or a triplet electronic state (T_1). In the former case the non-radiative transition is called internal conversion (IC)

* Corresponding author at: Key Laboratory of Organic Solids, Beijing National Laboratory for Molecular Science (BNLMS), Institute of Chemistry, Chinese Academy of Sciences, 100190 Beijing, PR China.
E-mail addresses: zgshuai@tsinghua.edu.cn, zgshuai@iccas.ac.cn (Z. Shuai).

0301-0104/$ - see front matter © 2010 Elsevier B.V. All rights reserved.
doi:10.1016/j.chemphys.2010.03.004

and in the latter case, the intersystem conversion (ISC). In contrast to radiative decay, the calculation of non-radiative decay rate is difficult mainly because the coupling between the electron and vibration is not simple. The non-adiabatic quantum dynamic theory is only limited to small molecules with two or three atoms [22,23] because it is impossible to obtain the potential energy surfaces for both excited state and ground state for polyatomic molecules. The displaced harmonic oscillator approximation model was first outlined by Robinson and Frosch [24]. Then the concepts and theory of radiationless transition in isolated molecules were first formulated in the 60s [25–34]. It has been widely applied to diatomic molecules at the *ab initio* quantum chemistry level [35,36]. Displaced harmonic oscillators model have been considered for small polyatomic molecules with limited DRE mode mixing by Lin et al. [37,38]. Recently Peng et al. derived an analytic internal conversion (IC) rate including complete mode mixing DRE [39]. Niu et al. further developed a more general promoting-mode free formula for IC rate [40]. In this work, we will first summarize these recent progresses and will present some numerical computational studies on the emission spectrum of anthracene and we will give a numerical rationalization for the exotic aggregation induced emission phenomena in 9-[(o-Aminophenyl)phenylmethylene]-9H-fluorene.

2. Methodology

2.1. Displaced harmonic oscillator model

Under the adiabatic approximation, the state of a molecule can be described a product of electronic state and vibrational state as $|j v_j\rangle = |\Phi_j\rangle|\Theta_{jv_j}\rangle$. In the harmonic approximation, the vibrational state is composed of $N = 3n - 6$ or $3n - 5$ (n is the number of atoms for a molecule) normal modes, $|\Theta_{jv_j}\rangle = |\chi_{jv_{j1}}\chi_{jv_{j2}}\cdots\chi_{jv_{jN}}\rangle$. And $v_j = \{v_{j1}, v_{j2}, \ldots, v_{jN}\}$ is a set of vibrational quantum numbers. $|\chi_{jv_{jk}}\rangle$ is the eigenstate of 1-dimensional harmonic oscillator Hamiltonian:

$$\widehat{H}_{jk} = \frac{1}{2}\left(\widehat{P}_{jk}^2 + \omega_{jk}^2\widehat{Q}_{jk}^2\right) \tag{1}$$

$\widehat{P}_{jk}$ and $\widehat{Q}_{jk}$ are the kth mass-weighted nuclear normal momentum operator and normal coordinate operator of the jth electronic state, respectively. And the initial and final electronic states are denoted by i and f. Then the normal coordinates of the two electronic states Q_{ik} and Q_{fl} are related by an orthogonal Duschinsky [41] rotation matrix $\mathbf{S}_{i\leftarrow f}$ and a displacement vector $\underline{D}_{i\leftarrow f}$ between the minima of the initial state and final state parabolas

$$Q_{ik} = \sum_l^N S_{i\leftarrow f,kl}Q_{fl} + \underline{D}_{i\leftarrow f,k} \tag{2}$$

In the following, we will conveniently abbreviate $\mathbf{S}_{i\leftarrow f}$ $\underline{D}_{i\leftarrow f}$ to $\mathbf{S}$ and $\underline{D}$.

2.2. Spontaneous radiative decay rate

In the framework of quantum electrodynamics, the spontaneous radiative decay rate per unit frequency range can be expressed as [42]

$$I_r(\omega) = \frac{4\omega^3}{3\hbar c^3}\sum_{v_i,v_f} P_{iv_i}(T)|\langle\Theta_{fv_f}|\vec{\mu}_{fi}|\Theta_{iv_i}\rangle|^2\delta(\omega_{iv_i fv_f} - \omega) \tag{3}$$

Here c is the vacuum velocity of light. $P_{iv_i}(T)$ is the Boltzmann distribution function for the initial vibronic manifold. $\vec{\mu}_{fi} = \langle\Phi_f|\vec{\mu}|\Phi_i\rangle$ is the electronic transition dipole moment, which depends on the nuclear coordinates, and can be expanded as

$$\vec{\mu}_{fi} = \vec{\mu}_0 + \sum_k \vec{\mu}_k Q_k + \sum_{k,l}\vec{\mu}_{kl}Q_kQ_l + \cdots \tag{4}$$

For strongly allowed transitions, the emission is usually dominated by the zero-order term, the first term of Eq. (4). While for weakly allowed or forbidden transition one must consider also the first order term, namely, the Herzberg–Teller approximation

$$\vec{\mu}_{fi} = \vec{\mu}_0 + \sum_k \vec{\mu}_k Q_k \tag{5}$$

Inserting (5) into (3), the rate formula turns into three parts,

$$I_r(\omega) = I_r^{\mathrm{FC}}(\omega) + I_r^{\mathrm{FC/HT}}(\omega) + I_r^{\mathrm{HT}}(\omega), \tag{6}$$

where

$$I_r^{\mathrm{FC}}(\omega) = \frac{4\omega^3}{3\hbar c^3}|\vec{\mu}_0|^2\sum_{v_i,v_f}P_{iv_i}(T)|\langle\Theta_{fv_f}|\Theta_{iv_i}\rangle|^2\delta(\omega_{iv_i fv_f} - \omega) \tag{7}$$

is the Franck–Condon (FC) spectrum, and

$$I_r^{\mathrm{FC/HT}}(\omega) = \frac{4\omega^3}{3\hbar c^3}\sum_{v_i,v_f}P_{iv_i}(T)\delta(\omega_{iv_i fv_f} - \omega)\sum_{k=1}^N\vec{\mu}_0\cdot\vec{\mu}_k\langle\Theta_{fv_f}|\Theta_{iv_i}\rangle \times\langle\Theta_{iv_i}|Q_{fk}|\Theta_{fv_f}\rangle \tag{8}$$

is the mixed spectrum of Franck–Condon and Herzberg–Teller, and

$$I_r^{\mathrm{HT}}(\omega) = \frac{4\omega^3}{3\hbar c^3}\sum_{v_i,v_f}P_{iv_i}(T)\delta(\omega_{iv_i fv_f} - \omega) \times\sum_{k,l=1}^N\vec{\mu}_k\cdot\vec{\mu}_l\langle\Theta_{fv_f}|Q_{fk}|\Theta_{iv_i}\rangle\langle\Theta_{iv_i}|Q_{fl}|\Theta_{fv_f}\rangle \tag{9}$$

is the Herzberg–Teller (HT) spectrum term.

Applying the Fourier transformation,

$$\delta(\omega) = \frac{1}{2\pi}\int e^{i\omega t}\,\mathrm{d}t \tag{10}$$

Eq. (7)–(9) can be recast as,

$$I_r^{\mathrm{FC}}(\omega) = \frac{2\omega^3}{3\pi\hbar c^3}|\vec{\mu}_0|^2\int e^{-i\omega t}e^{iE_{if}t/\hbar}Z_{iv}^{-1}\rho_0^{\mathrm{FC}}(t,T)\,\mathrm{d}t \tag{11}$$

$$I_r^{\mathrm{FC/HT}}(\omega) = \frac{2\omega^3}{3\pi\hbar c^3}\sum_k\vec{\mu}_0\cdot\vec{\mu}_k\int e^{-i\omega t}e^{iE_{if}t/\hbar}Z_{iv}^{-1}\rho_k^{\mathrm{FC/HT}}(t,T)\,\mathrm{d}t \tag{12}$$

$$I_r^{\mathrm{HT}}(\omega) = \frac{2\omega^3}{3\pi\hbar c^3}\sum_{k,l}\vec{\mu}k\cdot\vec{\mu}l\int e^{-i\omega t}e^{iE_{if}t/\hbar}Z_{iv}^{-1}\rho_{kl}^{\mathrm{HT}}(t,T)\,\mathrm{d}t \tag{13}$$

where

$$\rho_0^{\mathrm{FC}}(t,T) = \mathrm{Tr}\left[e^{-i\tau_f\widehat{H}_f}e^{-i\tau_i\widehat{H}_i}\right] \tag{14}$$

$$\rho_k^{\mathrm{FC/HT}}(t,T) = \mathrm{Tr}\left[Q_{fk}e^{-i\tau_f\widehat{H}_f}e^{-i\tau_i\widehat{H}_i}\right] \tag{15}$$

$$\rho_{kl}^{\mathrm{HT}}(t,T) = \mathrm{Tr}\left[Q_{fk}e^{-i\tau_f\widehat{H}_f}Q_{fl}e^{-i\tau_i\widehat{H}_i}\right] \tag{16}$$

are three correlation functions. Ianconescu and Pollak have first derived an analytic form of Eq. (14) by invoking Gaussian integrations:

$$\rho_0^{\mathrm{FC}}(t,T) = \sqrt{\frac{\det[\mathbf{a}_f\mathbf{a}_i]}{\det[\mathbf{B}]\det[\mathbf{B}-\mathbf{A}\mathbf{B}^{-1}\mathbf{A}]}} \times\exp\left\{\frac{i}{\hbar}[\underline{D}^T\mathbf{E}\mathbf{S}(\mathbf{B}-\mathbf{A})^{-1}\mathbf{G}\mathbf{S}^T\underline{D}]\right\}. \tag{17}$$

Here $\beta = 1/(k_BT)$, $\tau_f = t/\hbar, i\tau_i = \beta - i\tau_f, a_k(\tau) = \omega_k/\sin(\hbar\omega_k\tau), b_k(\tau) = \omega_k/\tan(\hbar\omega_k\tau)$. $\mathbf{a}$ and $\mathbf{b}$ are diagonal matrices, with diagonal elements $a_k(\tau)$, $b_k(\tau)$, respectively

$$\mathbf{A} = \mathbf{a}_f + \mathbf{S}^T\mathbf{a}_i\mathbf{S} \quad (18\text{-}1)$$
$$\mathbf{B} = \mathbf{b}_f + \mathbf{S}^T\mathbf{b}_i\mathbf{S} \quad (18\text{-}2)$$
$$\mathbf{G} = \mathbf{b}_f - \mathbf{a}_f \quad (18\text{-}3)$$
$$\mathbf{E} = \mathbf{b}_i - \mathbf{a}_i \quad (18\text{-}4)$$

In order to get a unified expression of Eq. (14)–(16), we define the following two matrices:

$$\mathbf{K} = \begin{bmatrix} \mathbf{B} & -\mathbf{A} \\ -\mathbf{A} & \mathbf{B} \end{bmatrix}_{2\times 2N} \quad (19\text{-}1)$$
$$\underline{F} = [\underline{D}^T\mathbf{E}\mathbf{S}\ \underline{D}^T\mathbf{E}\mathbf{S}]^T_{1\times 2N} \quad (19\text{-}2)$$

Then Eq. (17) can be rewritten as

$$\rho_0^{FC}(t,T) = \sqrt{\frac{\det[\mathbf{a}_f\mathbf{a}_i]}{\det[\mathbf{K}]}}\exp\left\{-\frac{i}{\hbar}\left[\frac{1}{2}\underline{F}^T\mathbf{K}\underline{F} - \underline{D}^T\mathbf{E}\underline{D}\right]\right\} \quad (20)$$

For FC/HT mixed spectrum term, an additional vector $\underline{H}_k^{FC/HT} = [0_1\cdots 1_k\cdots 0_{2N}]^T_{1\times 2N}$ is introduced. Then Eq. (15) can be written as,

$$\rho_k^{FC/HT}(t,T) = -\rho_0^{FC}(t,T)\left\{(\underline{H}_k^{FC/HT})\mathbf{K}^{-1}\underline{F}\right\} \quad (21)$$

For HT spectrum, a matrix $\mathbf{G}_{lk}^{HT} = \begin{bmatrix} 0_{11} & 0_{12} & \cdots & 0_{1N+l} & \cdots \\ 0_{21} & 0_{22} & \cdots & 0_{2N+l} & \cdots \\ \cdots & \cdots & \cdots & \cdots & \cdots \\ 0_{k1} & 0_{k2} & \cdots & 1_{kN+l} & \cdots \\ \cdots & \cdots & \cdots & \cdots & \cdots \end{bmatrix}$ is introduced so that the HT term Eq. (16) becomes

$$\rho_{kl}^{HT}(t,T) = \rho_0^{FC}(t,T)\left\{i\hbar\mathrm{Tr}[\mathbf{G}_{lk}^{HT}\mathbf{K}^{-1}] + (\mathbf{K}^{-1}\underline{F})^T\mathbf{G}_{lk}^{HT}(\mathbf{K}^{-1}\underline{F})\right\} \quad (22)$$

We further define,

$$\tilde{\mu}_r^2(t,T) = |\vec{\mu}_0|^2 - \sum_k \vec{\mu}_0\cdot\vec{\mu}_k\left[(\underline{H}_k^{FC/HT})\mathbf{K}^{-1}\underline{F}\right] + \sum_{kl}\vec{\mu}_k\cdot\vec{\mu}_l\left[i\hbar\mathrm{Tr}\left[\mathbf{G}_{lk}^{HT}\mathbf{K}^{-1}\right] + (\mathbf{K}^{-1}\underline{F})^T\mathbf{G}_{lk}^{HT}(\mathbf{K}^{-1}\underline{F})\right] \quad (23)$$

The final radiative decay rate per unit frequency range at ω can be obtained as:

$$I_r(\omega) = \frac{2\omega^3}{3\pi\hbar c^3}\int e^{-i\omega t}e^{iE_{ij}t/\hbar}Z_{iv}^{-1}\rho_0^{FC}(t,T)\tilde{\mu}_r^2(t,T)\,dt \quad (24)$$

The emission spectrum is closed related with Eq. (24):

$$I_r(\omega)\cdot\hbar\omega = \frac{2\omega^4}{3\pi c^3}\int e^{-i\omega t}e^{iE_{ij}t/\hbar}Z_{iv}^{-1}\rho_0^{FC}(t,T)\tilde{\mu}_r^2(t,T)\,dt \quad (25)$$

The spontaneous radiative decay rate constant is the integration of Eq. (24):

$$k_r = \int_0^\infty I_r(\omega)d\omega = k_r^{FC} + k_r^{FC/HT} + k_r^{HT} \quad (26)$$

Besides, the absorption coefficient of the absorption spectrum has the same form and derivation as the spontaneous emission spectrum, and the final calculation formula is

$$\alpha(\omega) = \frac{2\pi\omega}{3\hbar c}\int e^{i\omega t}e^{-iE_{fi}t/\hbar}Z_{iv}^{-1}\rho_0^{FC}(t,T)\tilde{\mu}_a^2(t,T)\,dt \quad (27)$$

2.3. Internal conversion (IC) rate

Applying Fermi Golden rule, the IC rate can be presented as,

$$k_{ic} = \frac{2\pi}{\hbar}|H'_{fi}|^2\delta(E_{fi} + E_{fv_f} - E_{iv_i}), \quad (28)$$

where

$$H'_{fi} = -\hbar^2\sum_l\left\langle\Phi_f\Theta_{fv_f}\left|\frac{\partial\Phi_i}{\partial Q_{fl}}\frac{\partial\Theta_{iv_i}}{\partial Q_{fl}}\right.\right\rangle$$

is the non-adiabatic perturbation. Applying Condon approximation,

$$H'_{fi} = -\hbar^2\sum_l\langle\Phi_f|\hat{P}_{fl}|\Phi_i\rangle\langle\Theta_{fv_f}|\hat{P}_{fl}|\Theta_{iv_i}\rangle \quad (29)$$

Substituting (29) into (28), the IC rate can be expressed as [40]

$$k_{ic} = \sum_{kl}\frac{2\pi}{\hbar}R_{kl}Z_{iv}^{-1}\sum_{v_i,v_f}e^{-\beta E_{iv_i}}P_{kl}\delta(E_{fi} + E_{fv_f} - E_{iv_i}) \quad (30)$$

Here

$$R_{kl} = \langle\Phi_f|\hat{P}_{fk}|\Phi_i\rangle\langle\Phi_i|\hat{P}_{fl}|\Phi_f\rangle \quad (31\text{-}1)$$
$$P_{kl} = \langle\Theta_{fv_f}|\hat{P}_{fk}|\Theta_{iv_i}\rangle\langle\Theta_{iv_i}|\hat{P}_{fl}|\Theta_{fv_f}\rangle \quad (31\text{-}2)$$

Using Fourier transformation of delta function,

$$k_{ic,kl} = \frac{1}{\hbar^2}R_{kl}\int_{-\infty}^{\infty}dt\left[e^{i\omega_{if}t}Z_{iv}^{-1}\rho_{ic,kl}(t,T)\right] \quad (32)$$

$\rho_{ic,kl}(t,T)$ is a correlation function of the form,

$$\rho_{ic,kl}(t,T) = \mathrm{Tr}\left[\hat{P}_{fk}e^{-i\tau_f\hat{H}_f}\hat{P}_{fl}e^{-i\tau_i\hat{H}_i}\right] \quad (33)$$

The analytic solution of the correlation function is obtained,

$$\rho_{ic,kl}(t,T) = \sqrt{\frac{\det[\mathbf{a}_f\mathbf{a}_i]}{\det[\mathbf{K}]}}\exp\left\{-\frac{i}{\hbar}\left[\frac{1}{2}\underline{F}^T\mathbf{K}^{-1}\underline{F} - \underline{D}^T\mathbf{E}\underline{D}\right]\right\}, \left\{i\hbar\mathrm{Tr}\left[\mathbf{G}_{lk}^{IC}\mathbf{K}^{-1}\right] + (\mathbf{K}^{-1}\underline{F})^T\mathbf{G}_{lk}^{IC}(\mathbf{K}^{-1}\underline{F}) - (\underline{H}_{kl}^{IC})^T\mathbf{K}^{-1}\underline{F}\right\} \quad (34)$$

where

$$\mathbf{G}_{lk}^{IC} = \begin{bmatrix} \mathbf{G}_{lk,11}^{IC} & \mathbf{G}_{lk,12}^{IC} \\ \mathbf{G}_{lk,21}^{IC} & \mathbf{G}_{lk,22}^{IC} \end{bmatrix}$$

$$\mathbf{G}_{lk,11}^{IC} = \begin{bmatrix} \cdots \\ 0 \\ -b_{fk}[\mathbf{S}^T\mathbf{a}_i\mathbf{S}]_{l\to k,:} \\ 0 \\ \cdots \end{bmatrix}$$

$$\mathbf{G}_{lk,12}^{IC} = \begin{bmatrix} \cdots \\ 0 \\ b_{fk}[\mathbf{S}^T\mathbf{b}_i\mathbf{S}]_{l\to k,:} \\ 0 \\ \cdots \end{bmatrix}$$

$$\mathbf{G}_{lk,21}^{IC} = \begin{bmatrix} \cdots \\ 0 \\ a_{fk}[\mathbf{S}^T\mathbf{a}_i\mathbf{S}]_{l\to k,:} \\ 0 \\ \cdots \end{bmatrix}$$

$$\mathbf{G}_{lk,22}^{IC} = \begin{bmatrix} \cdots \\ 0 \\ -a_{fk}[\mathbf{S}^T\mathbf{b}_i\mathbf{S}]_{l\to k,:} \\ 0 \\ \cdots \end{bmatrix}$$

$$\underline{H}_{kl}^{IC} = \begin{bmatrix} \underline{H}_{kl,1}^{IC} \\ \underline{H}_{kl,2}^{IC} \end{bmatrix}$$

$$\underline{H}_{kl,1}^{IC} = [\cdots\ 0\ \ b_{fk}[\underline{D}^T\mathbf{E}\mathbf{S}]_{l\to k}\ \ 0\ \ \cdots]^T$$

$$\underline{H}_{kl,2}^{IC} = [\cdots\ 0\ \ -a_{fk}[\underline{D}^T\mathbf{E}\mathbf{S}]_{l\to k}\ \ 0\ \ \cdots]^T$$

Here, $[\mathbf{S}^T\mathbf{a}_i\mathbf{S}]_{l\to k,:}$ is the lth row of matrix $[\mathbf{S}^T\mathbf{a}_i\mathbf{S}]$. We multiply it with $-b_{fk}$, and insert it into the kth row of $\mathbf{G}^{IC}_{lk,11}$. The rest rows of $\mathbf{G}^{IC}_{lk,11}$ are null. $[\underline{D}^T\mathbf{ES}]_{l\to k}$ is the lth element of row matrix $[\underline{D}^T\mathbf{ES}]$. We multiply it with b_{fk}, and then insert it into the kth row of $\underline{H}^{IC}_{kl}$, the rest elements of $\underline{H}^{IC}_{kl}$ are null.

Comparing IC correlation function Eq. (34) with HT correlation functions Eq. (21) and Eq. (22), it can be found that these have the same form. The only differences are the definition of matrix **G** and vector *H*.

The electronic coupling term R_{kl} of IC rate Eq. (30) can be obtained with the first order perturbation theory following Lin [25]. The electronic Hamiltonian can be expanded to the first order in a Taylor series of normal coordinates,

$$H = H_0 + \sum_k (\partial V/\partial Q_{fk})_0 Q_{kl}, \tag{35}$$

where H_0 contains the usual kinetic and potential energies for the electrons at the equilibrium configuration, $V \equiv V(\mathbf{r},\mathbf{R})$ stands for the Coulomb interaction potential between electrons and nuclei. The initial and final electronic states in the internal conversion process can be written as,

$$|\Phi_i\rangle \approx |\Phi_i^0\rangle + \sum_{j(\neq i)} \frac{\langle\Phi_j^0|\sum_k(\partial V/\partial Q_{fk})_0 Q_{fk}|\Phi_i^0\rangle}{(E_i^0 - E_j^0)}\left|\Phi_j^0\right\rangle, \tag{36}$$

$$|\Phi_f\rangle \approx \left|\Phi_f^0\right\rangle + \sum_{j(\neq f)} \left[\frac{\langle\Phi_j^0|\sum_k(\partial V/\partial Q_{fk})_0 Q_{fk}|\Phi_f^0\rangle}{(E_f^0 - E_j^0)}\right]\left|\Phi_j^0\right\rangle, \tag{37}$$

respectively.

Here E_i^0 and E_f^0 represent the adiabatic energy of two electronic states at the equilibrium position in the ground state. And the electronic coupling term can be obtained as,

$$\left\langle \Phi_f\left|\frac{\partial}{\partial Q_{fl}}\right|\Phi_i\right\rangle = \frac{\left\langle\Phi_f^0\left|\frac{\partial V}{\partial Q_{fl}}\right|\Phi_i^0\right\rangle}{(E_i^0 - E_f^0)}. \tag{38}$$

and the numerator can be expanded in the following way:

$$\begin{aligned}\frac{\partial V}{\partial Q_{fl}} &= -\sum_{\sigma,\alpha}\frac{\partial}{\partial Q_{fl}}\frac{Z_\sigma e^2}{|\mathbf{r}_\alpha - \mathbf{R}_\sigma|} \\ &= \sum_{\sigma,\alpha}\sum_j \frac{1}{\sqrt{M_\sigma}}\frac{\partial q_{\sigma j}}{\partial Q_{fl}}\frac{Z_\sigma e^2(r_{\alpha j} - R_{\sigma j})}{|\mathbf{r}_\alpha - \mathbf{R}_\sigma|^3} \\ &= -\sum_\sigma \frac{Z_\sigma e^2}{\sqrt{M_\sigma}}\sum_j E_{\sigma j}L_{f\sigma j,k}\end{aligned} \tag{39}$$

where α and σ are indices for electrons and nucleus, respectively. $j = x, y, z$ represents Cartesian component. $L_{f\sigma j,l} = \partial q_{\sigma j}/\partial Q_{fl}$ is the component of the kth eigenvector of Hessian matrix. $E_{\sigma j} = \sum_\alpha e(r_{\alpha j} - R_{\sigma j})/|\mathbf{r}_\alpha - \mathbf{R}_\sigma|^3$ is the jth component of the electric field operator for the nucleus centered at σ.

Then

$$\begin{aligned}\left\langle\Phi_f^0|\partial V/\partial Q_{fl}|\Phi_i^0\right\rangle &= -\sum_\sigma\frac{Z_\sigma e^2}{\sqrt{M_\sigma}}\sum_j\left\langle\Phi_f^0|E_{\sigma j}|\Phi_i^0\right\rangle L_{f\sigma j,l} \\ &\equiv -\sum_\sigma\frac{Z_\sigma e^2}{\sqrt{M_\sigma}}\sum_j E_{f\leftarrow i,\sigma j}L_{f\sigma j,k}\end{aligned} \tag{40}$$

$E_{f\leftarrow i,\sigma j}$ is the transition matrix element over the one-electron electric field (from all electrons) operator at atomic center σ. $E_{f\leftarrow i,\sigma j}$ can be calculated by CIS, TDDFT, or CASSCF methods which has already been implemented in quantum chemistry package such as Gaussian or Molpro.

3. Computational results for the photophysical properties of complex molecules

3.1. Computational details

The molecular equilibrium geometries for the ground state S_0 are optimized at the level of density functional theory (DFT) with hybrid exchange–correlation functional. And the time-dependent density functional theory (TDDFT) is applied to optimize the first excited S_1 state of the compounds. The B3LYP functional and 6-31g* basis set are used. At the equilibrium geometries, the vibrational frequencies and the normal vibrational modes of S_0 electronic states are calculated by analytic energy gradients, and the ones for S_1 are obtained by numerical energy gradients. These electronic structure calculations are carried out by using TURBOMOLE 5.9 program package [43]. The transition electric field $E_{f\leftarrow i,\sigma j} = \int \mathbf{dr}\rho_{fi}(\mathbf{r})E_{\sigma j}(\mathbf{r})$ ($\rho_{fi}(\mathbf{r})$ is the transition density) for each atom at the ground equilibrium geometry is calculated at the TDDFT/B3LYP/6-31G* level using Gaussian 03 program package [44] in order to calculate the electronic coupling terms for the IC process, namely, the first-order derivative of the excited state wavefunction with respect to the normal mode coordinates, see Ref. [39]. Based on the electronic structure information, the Duschinsky matrix and the normal mode displacements of the two electronic states of compounds, the radiative and non-radiative rate are evaluated by means of home-made codes.

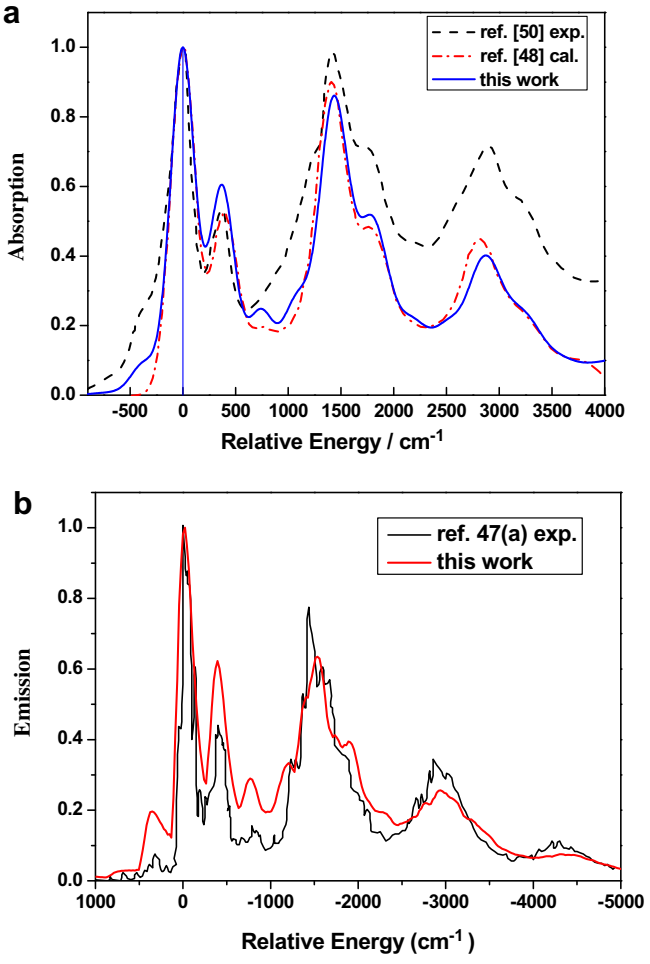

Fig. 1. Comparisons of the calculated absorption (a) and emission (b) spectra with the previous experiments and theoretical results (absorption only).

3.2. Spectra and rates of anthracene

We choose anthracene as the first example because (i) its photophysical properties are well-established [45], which can allow us to validate our formalism by comparing with previously reported results [2,15,46,47]; (ii) it is a typical member of rigid polycyclic aromatic hydrocarbons which shows interesting photophysical properties and from which many excellent opto-electronic materials can be derived. In order to compare the results, D_{2h} symmetry is adopted and the frequencies are scaled by the factor of 0.9614, which is a common practice [48]. The calculated vertical exited energies from S_0 ($1A_g$) to S_1 ($1B_{2u}$) are 3.23 eV, which is the same as previously calculated results [46], and the adiabatic excited energy (3.02 eV) also agrees well with the previous theoretical result (2.90 eV), while 0.41 eV lower than experimental one (3.43 eV [47]). Comparison of the obtained absorption and emission spectra with the experimental [49] as well as the previously calculated ones is shown in Fig. 1. The absorption spectrum is broadened by Gaussian function using a constant half-width of $\sigma = 100\ cm^{-1}$. From Fig. 1(a), it is clear that the computed absorption spectrum, including the weak shoulders located 300–750 cm^{-1} below the 0–0 transition corresponding to the hot band transitions, which was not manifested in Ref. [46], is in excellent agreement with the experiment. Fig. 1(b) shows that the calculated emission spectrum is also consistent with the experiment one. These indicate that our vibration correlation function method works very well for the molecular spectra. The radiative decay and the non-radiative IC rates are evaluated at 300 K. The radiative decay rate is calculated to be $2.28 \times 10^7\ S^{-1}$, which is close to previously documented experimental results of $6.20 \times 10^7\ S^{-1}$ in Ref. [50], or $5 \times 10^7\ S^{-1}$ in Ref. [2], or $6.0 \times 10^7\ S^{-1}$ in Ref. [47a]. The non-radiative decay rate is calculated to be $7.5 \times 10^5\ S^{-1}$, again comparable with experimental measurement of $3.5 \times 10^5\ S^{-1}$ from Ref. [50]. The nice agreements with the experiments validate the present efficient rate theory.

3.3. Aggregation induced emission phenomena in 9-[(o-Aminophenyl)phenylmethylene]-9H-fluorene molecule

In general, intermolecular interaction quenches luminescence. However, recently a class of molecules is found to exhibit exotic aggregation induced light emission phenomena, namely, the molecule is weakly luminescent in solution, but strongly emissive in aggregate forms [51]. A recent example is 9-[(o-Aminophenyl)phenylmethylene]-9H-fluorene (for molecular structure, see Fig. 2), which exhibit typical aggregation induced emission (AIE) behavior [52], much as many other systems [53–62]. AIE phenomenon has attracted much attention because a light-emitting device should work efficiently in solid phase. In order to understand the origin of the AIE phenomenon, we have performed first-principles calculations on the excited state decay rates in invoking the excited state-vibration couplings for silole [63,64], cis, cis-1, 2, 3, 4-tetraphenyl-1, 3-butadiene molecules [65], and phenyl substituted polyenes [66]. We found that (i) the non-radiative transition rate can be fully suppressed when going from solution phase to solid phase, because of the restriction of the side phenyl ring twisting motion; (ii) Duschinsky rotation effect is rather important in the photophysical process and essential to understand the temperature dependence of AIE molecules.

According to Jablonski diagram, there are three main pathways to dissipate energy from the first excited S_1 state: (i) the radiative process from S_1 to S_0 (k_r); (ii) the non-radiative internal conversion process from S_1 to S_0 (k_{nr}); (iii) the intersystem crossing process from S_1 to T_1 (k_{isc}). First, for the strongly fluorescent 9-[(o-Aminophenyl)phenylmethylene]-9H-fluorene molecule, k_{isc} is very small and can be neglected owing to small spin–orbital coupling constant in pure organic systems, while the IC rate of such flexible system becomes much faster than that of the rigid planar molecule (say anthracene) due to the ease of energy dissipation through vibration in the flexible molecules and the intersystem crossing

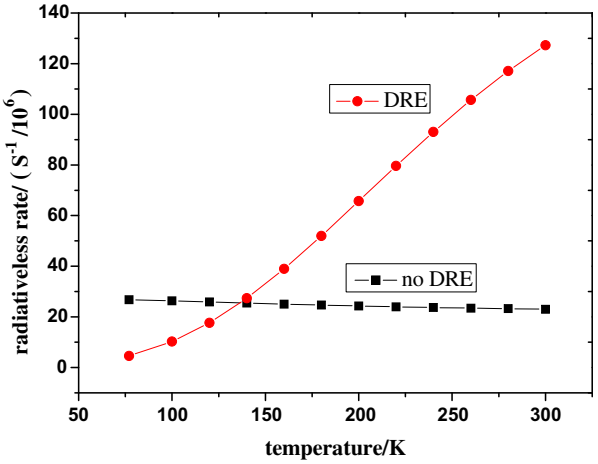

Fig. 3. Temperature dependence of internal conversion rates of the radiationless transition from S_1 to S_0 states of 9-[(o-Aminophenyl)phenylmethylene]-9H-fluorene: with DRE (filled circle) and without DRE (filled square).

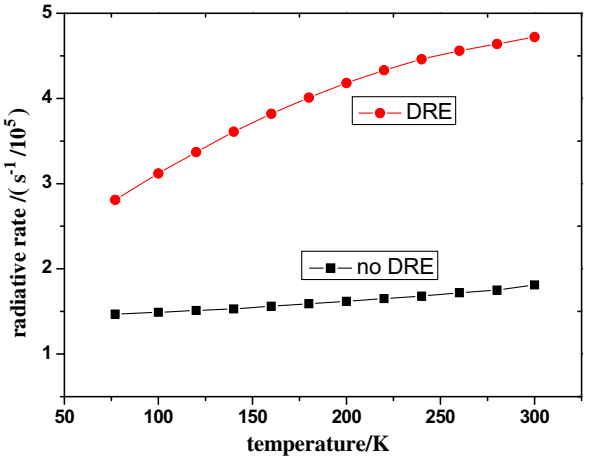

Fig. 4. Temperature dependence of the radiative transition rates from S_1 to S_0 states of 9-[(o-Aminophenyl)phenylmethylene]-9H-fluorene: with DRE (filled circle) and without DRE (filled square).

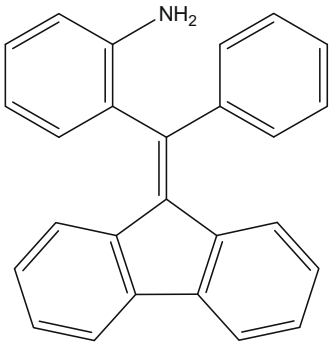

Fig. 2. Molecular structure of 9-[(o-Aminophenyl)phenylmethylene]-9H-fluorene molecule.

process can not compete. Thus we will focus on the IC and the radiative rates.

Figs. 3 and 4 present the calculated temperature dependence of the radiative decay and IC rates with and without DRE for 9-[(o-Aminophenyl)phenylmethylene]-9H-fluorene. The following observations can be made: (i) taking DRE into account, the IC rate is calculated to increase about 30 times from 77 K to 300 K. If DRE is neglected, the IC rate does not really depend on temperature; (ii) the radiative decay rates are hardly dependent on temperature, with DRE or without DRE; (iii) If DRE is ignored, k_{IC} at any temperature is always more than 200 times larger than k_r which is contrary to experiment. When DRE is considered, at low temperature (77 K), k_{IC} is about 20 times as large as k_r, but becomes almost three orders of magnitudes larger at 300 K, indicating temperature fluorescence quenching phenomena, in agreement with experiment.

Normal modes contribute in two parts to the excited state decay processes: in the electronic coupling term $R_{kl} = \langle \Phi_f | \hat{P}_{fk} | \Phi_i \rangle \langle \Phi_i | \hat{P}_{fl} | \Phi_f \rangle$ appearing in the prefactor of IC rate formula and in the Franck–Condon factor for both rate formulae representing the contributions from the normal reorganization energy going from one electronic state to another. We present some normal modes with noticeable contributions for the S_0 and S_1 states in Table 1.

The calculated electronic coupling matrix R_{kl} is plotted in Fig. 5. Note that the present formalism is promoting-mode free, namely, all the modes contribute to promote the internal conversion process through the matrix R_{kl} form. From Fig. 5, it can be seen that the matrix elements with larger values always involve the double-bond stretching vibrations of carbon–carbon, with frequencies $\sim$1600 cm^{-1}(indexed $\sim$ 100 in the normal mode ascending sequence). It is also noted that this mode couples strongly with many others modes. Thus, even though one can identify one mode with the largest contribution, only considering R_{kk} ($k \sim 100$) in the tradi-

Table 1
Wavenumber (cm^{-1}) of normal modes with non-negligible contribution for the S_0 and S_1 states.

Mode	S_0	S_1
1	21	42
2	33	56
3	45	62
4	51	77
5	61	81
6	70	101
7	103	118
9	160	170
11	192	191
12	201	200
13	228	233
17	303	311
18	351	397
19	405	429
20	421	434
21	427	437
22	440	455
24	462	465
28	520	544
29	551	551
30	557	568
31	585	578
33	614	595
38	703	665
40	724	717
41	759	749
42	762	756
44	771	767
46	785	801
49	835	835
53	884	889
57	966	960
58	975	964
60	987	976
63	1013	999
68	1048	1034
71	1062	1052
72	1078	1053
74	1106	1107
76	1151	1142
82	1191	1196
83	1220	1220
85	1258	1249
86	1291	1299
90	1338	1341
91	1342	1351
96	1477	1432
99	1490	1486
100	1513	1492
103	1532	1517
104	1617	1534
107	1633	1601
109	1642	1610
112	1666	1640
113	1669	1657
114	3154	3155
119	3172	3166
123	3181	3182
124	3185	3186
130	3225	3208
131	3538	3415

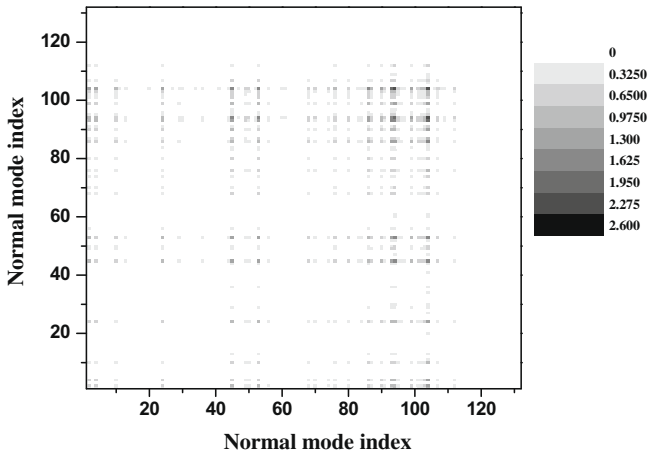

Fig. 5. The electronic coupling matrix elements R_{kl}.

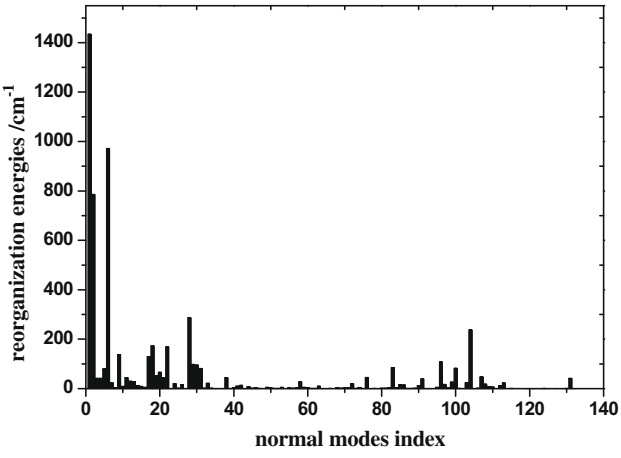

Fig. 6. The calculated reorganization energy for each normal mode for 9-[(o-Aminophenyl)phenylmethylene]-9H-fluorene.

tional promoting mode formalism is incomplete, because many other non-diagonal terms could be also important.

For a normal mode l, its reorganization energy λ_l is the product of the Huang–Rhys factor ($HR_l = \frac{\omega_l \times D_l^2}{2\hbar}$) of the normal mode and the corresponding vibrational energy $\hbar\omega_l$, $\lambda_l = HR_l \times \hbar\omega_l$, seen in Fig. 6. The normal modes are indexed with increasing frequencies.

The first six low-frequency modes (<100 cm^{-1}) contribute largely to the reorganization energy, about 56% of the total. According to our previous work [63–66], this could lead to aggregation induced emission phenomena, namely, energy dissipation pathways via low-frequency (twisting or group-swinging) motions are easily quenched in aggregation or at lower temperature, leading to radiative decay recovery.

We further look in detail the Duschinsky rotation matrix, which manifests the difference between the potential energy surfaces of electronic excited state and ground state at the harmonic oscillator approximation. The contour map for the absolute values of the Duschinsky rotation matrix elements is depicted in Fig. 7. The absolute values of matrix elements can measure the mixing degree of the corresponding two modes of two electronic states. Fig. 7(a) indicates that the mixing of the first six modes with low frequencies (<100 cm^{-1}) is large. Therefore, from the above two points, a conclusion can be drawn that the low-frequency modes, which correspond to the twist motions of two free phenyl rings, are very important in the process of non-radiatively dissipating the excited state energy. Moreover, this suggests that DRE can have great effect on the IC rate. Besides, from Fig. 7(b), it can be seen that apart from the low-frequency modes, the Duschinsky rotation matrix is almost diagonal, which means that the mode mixings for all other modes are negligible.

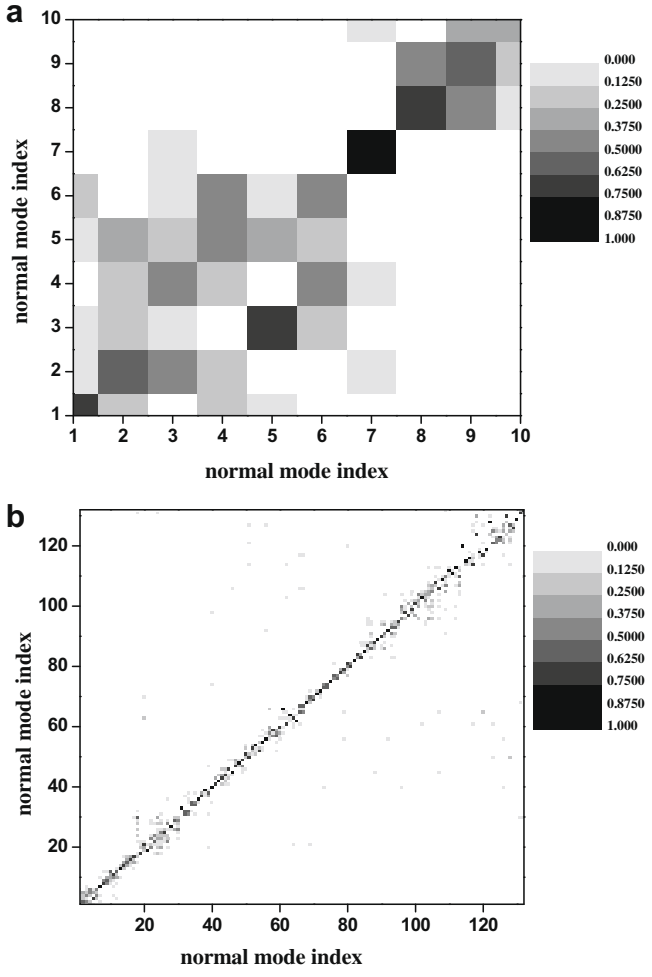

Fig. 7. Contour map of Duschinsky rotation matrix. (a) for the first six normal modes; (b) for all the normal modes in 9-[(o-Aminophenyl)phenylmethylene]-9H-fluorene molecule.

4. Summary

To summarize, we have developed the general analytic radiative and non-radiative decay rate formalism with Herzberg–Teller and Duschinsky rotation effects through vibration correlation function approach. The advantages of the present rate theory are that (i) the formalism is analytic and general which can be easily implemented numerically in coupling with modern electronic structure theory; (ii) it can be applied to quantitatively understand the photophysics of complex molecules. The application to anthracene shows that the calculated absorption and emission spectra and the radiative and non-radiative decay rates are all in good agreement with the experiments. To the best of our knowledge, this is the first theoretical calculation at the first-principles level. Then we interpret the exotic aggregation induced emission phenomenon for 9-[(o-Aminophenyl)phenylmethylene]-9H-fluorene: the combination of the twisting motions of free phenyl rings (largely contributing to nuclear motion part) and the double-bond stretching vibrations (largely contributing to electronic coupling part) largely dissipates the energy of the excited state, which leads to the compound no luminescence in diluted organic solution. However, the motions are easily suppressed in molecular aggregation state at low temperature or with high water contents of solution, and the non-radiative decay channel is blocked. Then the radiative decay dominates and the fluorescent efficiency is enhanced. The present rate theory is both an effective tool to describe the excited-states dynamic processes of large molecules and a powerful tool for the design of new high-efficiency light-emitting materials. It should be borne in mind that the displaced harmonic oscillator model is a quite crude approximation. It is valid for dynamics near the equilibrium point in the potential energy surface. Anharmonicity has been ignored here which could cause serious errors when deviating well away from the equilibrium points. We note that recent progresses in semiclassical on-the-fly approach by Tatchen and Pollak [67] could be very promising to overcoming such difficulty.

Acknowledgements

Many illuminating discussions with Professor Eli Pollak, Professor Jiushu Shao, and Professor Ben Zhong Tang are greatly acknowledged. It is our great pleasure to celebrate the 60th anniversary of our friend Eli by this contribution. This work is supported by the National Science Foundation of China and the Ministry of Science and Technology of China through 973 Program (Grant Nos. 2006CB806200, 2006CB932100, and 2009CB623600).

References

[1] (a) B.M. Krasovitskii, B.M. Bolotin, Organic Luminescent Materials, VCH: Weinheim, Germany, 1988;
(b) J. Shinar (Ed.), Organic Light-Emitting Devices, Springer, New York, 2004;
(c) N.H. Norton, Biomedical Sensors, Fundamentals, and Applications, Noys Publications, Park Ridge, NJ, 1982.
[2] N.J. Turro, Modern Molecular Photochemistry, Benjamin/Cummings Publishing Co., Inc., California, 1978.
[3] L.S. Cederbaum, W. Domcke, J. Chem. Phys. 64 (1976) 603.
[4] E.V. Doktorov, I.A. Malkin, V.I. Man'ko, J. Mol. Spectrosc. 64 (1977) 302.
[5] H. Kupkaand, P.H. Cribb, J. Chem. Phys. 85 (1986) 303.
[6] D. Grunerand, P. Brumer, Chem. Phys. Lett. 138 (1987) 310.
[7] M. Roche, Chem. Phys. Lett. 168 (1990).
[8] P.T. Ruhoff, Chem. Phys. 186 (1994) 355.
[9] R. Berger, C. Fischer, M. Klessinger, J. Phys. Chem. A 102 (1998) 7157.
[10] P.T. Ruhoffand, M.A. Ratner, Int. J. Quant. Chem. 77 (2000) 383.

[11] A. Hazraand, M. Nooijen, Int. J. Quant. Chem. 95 (2003) 643.
[12] G. Heimel, M. Daghofer, J. Gierschner, E.J.W. List, A.C. Grimsdale, K. Müllen, D. Beljonne, J.L. Brédas, E. Zojer, J. Chem. Phys. 122 (2005) 054501.
[13] Y.J. Yan, S. Mukamel, J. Chem. Phys. 85 (1986) 5908.
[14] M. Dierksen, S. Grimme, J. Chem. Phys. 122 (2005) 244101.
[15] S. Grimme, F. Neese, J. Chem. Phys. 127 (2007) 154116.
[16] F. Santoroa, R. Improta, A. Lami, J. Bloino, V. Barone, J. Chem. Phys. 126 (2007) 084509.
[17] F. Santoroa, A. Lami, R. Improta, V. Barone, J. Chem. Phys. 126 (2007) 184102.
[18] F. Santoroa, A. Lami, R. Improta, J. Bloino, V. Barone, J. Chem. Phys. 128 (2008) 224311.
[19] (a) E. Pollak, Y. He, J. Phys. Chem. B 105 (2001) 6500;
(b) Y. He, E. Pollak, J. Phys. Chem. A 105 (2001) 10961.
[20] (a) Y. He, E. Pollak, J. Chem. Phys. 116 (2002) 6088;
(b) R. Ianconescu, E. Pollak, J. Phys. Chem. A 108 (2004) 7778.
[21] J. Tatchen, E. Pollak, J. Chem. Phys. 128 (2008) 164303.
[22] F.J. Aoiz, L. Banares, J.F. Castillo, V.J. Herrero, B. Martinez-Haya, Phys. Chem. Chem. Phys. 4 (2002) 4379.
[23] N. Balucani, P. Casavecchia, F.J. Aoiz, L. Banares, J.F. Castillo, V.J. Herrero, Mol. Phys. 103 (2005) 1703.
[24] G.W. Robinson, R.P. Frosch, J. Chem. Phys. 37 (1962) 1962;
W. Robinson, R.P. Frosch, J. Chem. Phys. 38 (1963) 1187.
[25] S.H. Lin, J. Chem. Phys. 44 (1966) 3759.
[26] S.H. Lin, R. Bersohn, J. Chem. Phys. 48 (1968) 2732.
[27] S.H. Lin, J. Chem. Phys. 58 (1973) 5760.
[28] S.H. Lin, Proc. R. Soc. London, Ser. A 352 (1976) 57.
[29] M. Bixon, J. Jortner, J. Chem. Phys. 48 (1968) 715.
[30] M. Bixon, J. Jortner, J. Chem. Phys. 50 (1969) 3284;
M. Bixon, J. Jortner, J. Chem. Phys. 50 (1969) 4061.
[31] A. Nitzan, J. Jortner, J. Chem. Phys. 55 (1971) 1355.
[32] W. Siebrand, J. Chem. Phys. 54 (1971) 363.
[33] S. Fischer, Chem. Phys. Lett. 11 (1971) 577.
[34] D.F. Heller, K.F. Freed, W.M. Gelbart, J. Chem. Phys. 56 (1972) 2309.
[35] M.C. Van Hemert, H. Dohmann, S.D. Peyerimhoff, Chem. Phys. 110 (1986) 55.
[36] R. de Vivie, C.M. Marian, S.D. Peyerimhoff, Chem. Phys. 112 (1987) 349.
[37] M. Hayashi, A.M. Mebel, K.K. Liang, S.H. Lin, J. Chem. Phys. 108 (1998) 2044.
[38] A.M. Mebel, M. Hayashi, K.K. Liang, S.H. Lin, J. Phys. Chem. A 103 (1999) 10674.
[39] Q. Peng, Y.P. Yi, Z.G. Shuai, J.S. Shao, J. Chem. Phys. 126 (2007) 114302.
[40] Y.L. Niu, Q. Peng, Z.G. Shuai, Sci. China Ser. B-Chem. 51 (2008) 1153.
[41] F. Duschinsky, Acta Physicochim. URSS 7 (1937) 551.
[42] B. Dibartolo, Radiationless Processes, Plenu Press, New York, London, 1980.
[43] (a) P. Deglmann, F. Furche, R. Ahlrichs, Chem. Phys. Lett. 362 (2002) 511;
(b) P. Deglmann, F. Furche, J. Chem. Phys. 117 (2002) 9535.
[44] (a) B.G. Johnson, P.M.W. Gill, J.A. Pople, Chem. Phys. Lett. 206 (1993) 239;
(b) F. Furche, J. Chem. Phys. 114 (2001) 5982; (c) M.J. Frisch, G.W. Trucks, H.B. Schlegel, et al., Gaussian 03, Gaussion Inc., Carnegie, PA, 2003.
[45] (a) W.R. Lambert, P.M. Felker, A.H. Zewail, J. Chem. Phys. 75 (1981) 5958;
(b) W.R. Lambert, P.M. Felker, A.H. Zewail, J. Chem. Phys. 81 (1984) 2217;
(c) A.I. Novaria, V. Avila, G.G. Montich, C.M. Previtali, J. Photochem. Photobiol. B Biol. 60 (2001) 25;
(d) T.S. Ahn, A.M. Müller, R.O. Al-Kaysi, F.C. Spano, J.E. Norton, D. Beljonne, J.L. Brédas, C.J. Bardeen, J. Chem. Phys. 128 (2008) 054505;
(e) M. Baba, M. Saitoh, K. Taguma, K. Shinohara, K. Yoshida, Y. Semba, S. Kasahara, N. Nakayama, H. Goto, T. Ishimoto, U. Nagashima, J. Chem. Phys. 130 (2009) 134315.
[46] M. Dierksen, S. Grimme, J. Chem. Phys. 120 (2004) 3544.
[47] (a) J.B. Birks, Organic Molecular Photophysics, Bristol, England, 1973.;
(b) W.R. Lambert, P.M. Felker, J.A. Syage, A.H. Zewail, J. Chem. Phys. 81 (1984) 2195.
[48] W. Koch, M.C. Holthausen, A Chemist's Guide to Density Functional Theory, second ed., Wiley-VCH Verlag GmbH, 2001. p. 134.
[49] J. Ferguson, L.W. Reeves, W.G. Schneider, Can. J. Chem. 35 (1957) 1117.
[50] N. Nijegorodov, V. Ramachandran, D.P. Winkoun, Spectrochim. Acta Part A 53 (1997) 1813.
[51] J. Luo, Z. Xie, J.W.Y. Lam, L. Cheng, H. Chen, C. Qiu, H.S. Kwok, X. Zhan, Y. Liu, D. Zhu, B.Z. Tang, Chem. Commun. (2001) 1740.
[52] H. Tong, Y.Q. Dong, M. Häussler, Y. Hong, J.W.Y. Lam, H.H.Y. Sung, I.D. Williams, J.Z. Sun, B.Z. Tang, Chem. Commun. (2006) 1133.
[53] B.Z. Tang, X.W. Zhan, G. Yu, P.P.S. Lee, Y.Q. Liu, D.B. Zhu, J. Mater. Chem. 11 (2001) 2974.
[54] B.K. An, S.K. Kwon, S.D. Jung, S.Y. Park, J. Am. Chem. Soc. 124 (2002) 14410.
[55] J.W. Chen, C.C.W. Law, J.W.Y. Lam, Y.P. Dong, S.M.F. Lo, I.D. Williams, D.B. Zhu, B.Z. Tang, Chem. Mater. 15 (2003) 1535.
[56] J.W. Chen, B.K. An, D.S. Lee, J.S. Lee, Y.S. Park, H.S. Song, S.Y. Park, J. Am. Chem. Soc. 126 (2004) 10232.
[57] S.H. Lee, B.B. Jang, Z.H. Kafafi, J. Am. Chem. Soc. 127 (2005) 9071.
[58] F. Wang, M. Han, K.Y. Mya, Y. Wang, Y. Lai, J. Am. Chem. Soc. 127 (2005) 10350.
[59] M. Han, M. Hara, J. Am. Chem. Soc. 127 (2005) 10951.
[60] H. Tong, Y.Q. Dong, M. Häussler, Y. Hong, J.W.Y. Lam, H.H.Y. Sung, I.D. Williams, H.S. Kwok, B.Z. Tang, Chem. Phys. Lett. 428 (2006) 326.
[61] H. Tong, Y. Hong, Y.Q. Dong, M. Häussler, J.W.Y. Lam, Z. Li, Z.F. Guo, Z.H. Guo, B.Z. Tang, Chem. Commun. (2006) 3705.
[62] Q. Zeng, Z. Li, Y.Q. Dong, C.A. Di, A.J. Qin, Y.N. Hong, L. Ji, Z.C. Zhu, C.K.W. Jim, G. Yu, Q.Q. Li, Z.G. Li, Y.Q. Liu, J.G. Qin, B.Z. Tang, Chem. Commun. (2007) 70.
[63] G. Yu, S. Yin, Y. Liu, J. Chen, X. Xu, X. Sun, D. Ma, X. Zhan, Q. Peng, Z. Shuai, B.Z. Tang, D. Zhu, W. Fang, Y. Luo, J. Am. Chem. Soc. 127 (2005) 6335.
[64] S.W. Yin, Q. Peng, Z.G. Shuai, W.H. Fang, Y.H. Wang, Y. Luo, Phys. Rev. B 73 (2006) 205409.
[65] Q. Peng, Y.P. Yi, Z.G. Shuai, J.S. Shao, J. Am. Chem. Soc. 129 (2007) 9333.
[66] Q. Peng, Y.L. Niu, Z.G. Shuai, Chem. J. Chin. Univ. 29 (2008) 2435.
[67] J. Tatchen, Eli Pollak, J. Chem. Phys. 130 (2009) 041103.